



# Constraint of soil moisture on CO<sub>2</sub> efflux from tundra lichen, moss, and tussock in Council, Alaska, using a hierarchical Bayesian model

Y. Kim<sup>1</sup>, K. Nishina<sup>2</sup>, N. Chae<sup>3</sup>, S. J. Park<sup>4</sup>, Y. J. Yoon<sup>5</sup>, and B. Y. Lee<sup>5</sup>

<sup>1</sup>International Arctic Research Center, University of Alaska Fairbanks, AK 99775-7335, USA

<sup>2</sup>Center for Regional Environmental Research, National Institute for Environmental Studies, Tsukuba, 305-8506, Japan

<sup>3</sup>Civil and Environmental Engineering, Yonsei University, Seoul 120-749, South Korea

<sup>4</sup>Division of Climate Change, Korea Polar Research Institute (KOPRI), Incheon 406-840, South Korea

<sup>5</sup>Arctic Research Center, Korea Polar Research Institute (KOPRI), Incheon 406-840, South Korea

Correspondence to: Y. Kim (kimyw@iarc.uaf.edu)

Received: 3 March 2014 – Published in Biogeosciences Discuss.: 25 April 2014

Revised: 7 September 2014 – Accepted: 9 September 2014 – Published: 13 October 2014

**Abstract.** The tundra ecosystem is quite vulnerable to drastic climate change in the Arctic, and the quantification of carbon dynamics is of significant importance regarding thawing permafrost, changes to the snow-covered period and snow and shrub community extent, and the decline of sea ice in the Arctic. Here, CO<sub>2</sub> efflux measurements using a manual chamber system within a 40 m × 40 m (5 m interval; 81 total points) plot were conducted within dominant tundra vegetation on the Seward Peninsula of Alaska, during the growing seasons of 2011 and 2012, for the assessment of driving parameters of CO<sub>2</sub> efflux. We applied a hierarchical Bayesian (HB) model – a function of soil temperature, soil moisture, vegetation type, and thaw depth – to quantify the effects of environmental factors on CO<sub>2</sub> efflux and to estimate growing season CO<sub>2</sub> emissions. Our results showed that average CO<sub>2</sub> efflux in 2011 was 1.4 times higher than in 2012, resulting from the distinct difference in soil moisture between the 2 years. Tussock-dominated CO<sub>2</sub> efflux is 1.4 to 2.3 times higher than those measured in lichen and moss communities, revealing tussock as a significant CO<sub>2</sub> source in the Arctic, with a wide area distribution on the circumpolar scale. CO<sub>2</sub> efflux followed soil temperature nearly exponentially from both the observed data and the posterior medians of the HB model. This reveals that soil temperature regulates the seasonal variation of CO<sub>2</sub> efflux and that soil moisture contributes to the interannual variation of CO<sub>2</sub> efflux for the two growing seasons in question. Obvious changes in soil moisture during the growing seasons of 2011 and 2012 resulted in an explicit difference between CO<sub>2</sub> effluxes –

742 and 539 g CO<sub>2</sub> m<sup>-2</sup> period<sup>-1</sup> for 2011 and 2012, respectively, suggesting the 2012 CO<sub>2</sub> emission rate was reduced to 27 % (95 % credible interval: 17–36 %) of the 2011 emission, due to higher soil moisture from severe rain. The estimated growing season CO<sub>2</sub> emission rate ranged from 0.86 Mg CO<sub>2</sub> in 2012 to 1.20 Mg CO<sub>2</sub> in 2011 within a 40 m × 40 m plot, corresponding to 86 and 80 % of annual CO<sub>2</sub> emission rates within the western Alaska tundra ecosystem, estimated from the temperature dependence of CO<sub>2</sub> efflux. Therefore, this HB model can be readily applied to observed CO<sub>2</sub> efflux, as it demands only four environmental factors and can also be effective for quantitatively assessing the driving parameters of CO<sub>2</sub> efflux.

## 1 Introduction

Carbon dioxide (CO<sub>2</sub>) efflux from the soil surface into the atmosphere is important for estimating regional and global carbon budgets (Schlesinger and Andrews, 2000; Bond-Lamberty and Thomson, 2010), as well as being susceptible to increasing air temperature (Bond-Lamberty and Thomson, 2010), the degradation of permafrost (Schuur et al., 2009; Jensen et al., 2014), and the expansion of the shrub community (Sturm et al., 2005). All of which suggests the alteration of the terrestrial carbon cycle in response to drastic climate change in the Arctic (ACIA, 2004).

The tundra ecosystem of Alaska has received increased attention for the enhanced greening of abundant Arctic coastal

shrubs that has come with the decline of sea ice (Bhatt et al., 2010, 2013; Post et al., 2013), the shortened snow-covered period (Hinzman et al., 2005), thawing permafrost, and shrinking ponds and lakes (Romanovsky et al., 2002; Yoshikawa and Hinzman, 2003; Hinzman et al., 2005; Smith et al., 2005) – all of these reflect the changes in terrestrial carbon and water cycles (Davidson et al., 1998; Oechel et al., 2000; Michaelson and Ping, 2003; ACIA, 2004; Oberbauer et al., 2007; Walter et al., 2007; Koven et al., 2011). Recently, Jensen et al. (2014) found a distinct difference in CO<sub>2</sub> efflux from undisturbed tundra during 2011 and 2012, resulting from greater rainfall in the growing season of 2012. This suggests that higher soil moisture from rainfall is a suppressant factor for soil-produced CO<sub>2</sub> emitted into the atmosphere (Davidson et al., 1998; Oberbauer et al., 2007), decreasing CO<sub>2</sub> emissions by 43 % (Jensen et al., 2014). Davidson et al. (1998) reported that CO<sub>2</sub> efflux increased with soil moisture of 0 to 0.2 m<sup>3</sup> m<sup>-3</sup> and steadily decreased with increasing soil moisture content beyond 0.2 m<sup>3</sup> m<sup>-3</sup>. Hence, CO<sub>2</sub> efflux magnitude depends profoundly on the extent of soil moisture. Further, soil temperature is well-known as a significant factor in the regulation of CO<sub>2</sub> efflux in terrestrial ecosystems worldwide, as reported by many researchers (Davidson et al., 1998; Xu and Qi, 2001; Davidson and Janssens, 2006; Rayment and Jarvis, 2000; Kim et al., 2007, 2013; Jensen et al., 2014). The  $Q_{10}$  value, which is a measure of the change in reaction rate at intervals of 10 °C (Lloyd and Taylor, 1994), has been effectively used to evaluate the temperature sensitivity of soil microbial activity as an exponential function (Davidson et al., 1998; Xu and Qi, 2001; Monson et al., 2006; Bond-Lamberty and Thomson, 2010; Kim et al., 2013). For example, Monson et al. (2006) estimated their highest  $Q_{10}$  value,  $1.25 \times 10^6$ , as the beneath-snowpack soil temperature warmed from -3 to 0 °C in a high-elevation subalpine forest in Colorado, reflecting higher CO<sub>2</sub> production by beneath-snow microbes (such as snow molds) during the end of winter and early spring season. In the well-drained soil of Zackenberg, Greenland, higher CO<sub>2</sub> concentrations in frozen soil came from a soil-thawing spring burst event, related to the trapping of CO<sub>2</sub> produced during winter. Subsequently, there is a distinct difference in  $Q_{10}$  values between temperatures above and below zero;  $Q_{10}$  value below zero was 430, even when water content was 39 % (Elberling and Brandt, 2003). Therefore, soil temperature, which is an analogue of soil microbial activity under the assumption that soil moisture and substrate availability are not limiting factors, is the most important factor in producing CO<sub>2</sub> in the soil.

Monthly CO<sub>2</sub> efflux measured in the tundra ecosystem has been further recognized as having insufficient spatiotemporal resolution and efflux data representativeness from the conventional dynamic chamber method (Hutchinson and Livingston, 2002; Savage and Davidson, 2003). Oberbauer et al. (1992) developed a mathematical model which proved that soil temperature and water table depth might be used as efficient predictors of ecosystem CO<sub>2</sub> efflux in the ripar-

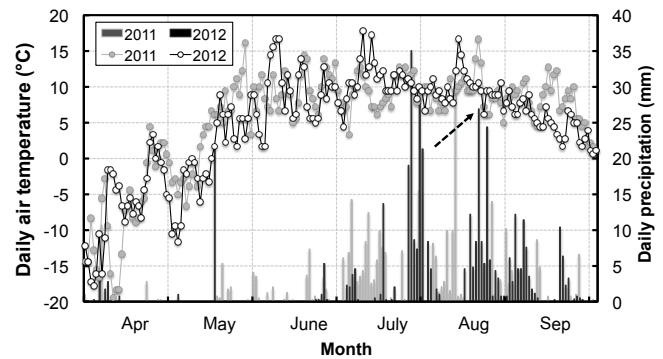


**Figure 1.** Average daily ambient temperature and precipitation in Council, Seward Peninsula, Alaska during April–October of 2011 and 2012 (Western Regional Climate Center). Dotted arrows denote that cumulative rainfall in 2012 exceeds that of 2011, beginning 20 August 2012.

ian tundra of the northern foothills of Alaska. In order to overcome the weakness of monthly CO<sub>2</sub> efflux measurement in the field, the hierarchical Bayesian (HB) model framework can be applied for the estimation of CO<sub>2</sub> efflux from the tundra ecosystem, as in Clark (2005) and Nishina et al. (2009, 2012). Their results indicated that the HB model is an effective tool for the estimation of fluxes and evaluation of parameters with less bias. Lately, free software such as WinBUGS (<http://www.mrc-bsu.ac.uk/bugs>) has resulted in the development of a HB model using the Markov Chain Monte Carlo (MCMC) method (Spiegelhalter and Best, 2000). Clark (2005) described that the HB model reveals complex nonlinear relationships between efflux and environmental factors.

In this study, we modeled observed CO<sub>2</sub> efflux using a HB model with four explanatory variables: soil temperature, soil moisture, vegetation types, and thaw depth, all under the assumption of the lognormal distribution. The HB model used in this study accommodated nonlinear relationships between efflux and environmental factors. Therefore, the objectives of this study are to (1) evaluate the effects of dominant plants on CO<sub>2</sub> efflux; (2) quantitatively assess driving parameters of CO<sub>2</sub> efflux simulated by a hierarchical Bayesian (HB) model; and (3) estimate growing season CO<sub>2</sub> emission rate within a 40 m × 40 m plot in the western Alaska tundra ecosystem.

## 2 Materials and methods

### 2.1 Study site and experimental methods

The study site is primarily covered by typical tussock tundra. This site is located at the community of Council (64°51′38.3″ N; 163°42′39.7″ W; 45 m a.s.l.) on the Seward Peninsula, about 120 km northeast of Nome, Alaska. This site was selected for its relatively smooth transition from

forest to tundra, with underlying discontinuous permafrost regime. The monthly average air temperature of 1.2 °C at the Nome airport from 1971 to 2010 ranged from −10.5 °C in January to 14.6 °C in July. Annual average precipitation was 427 mm, including snowfall (Western Regional Climate Center). During the growing seasons (June to September) of 2011 and 2012, average ambient temperature and precipitation were  $8.9 \pm 1.0$  °C (CV, coefficient of variance: 12 %) and 285 mm, and  $8.5 \pm 2.8$  °C (CV: 33 %) and 380 mm, respectively, as shown in Fig. 1. Precipitation in July–August of 2011 and 2012 were 231 and 299 mm, respectively, corresponding to 81 and 79 % of growing season precipitation. Under heavy precipitation in early July of 2011, CO<sub>2</sub> efflux measurement could not be conducted, unfortunately, due to the underestimation of CO<sub>2</sub> efflux. The sampling periods were June 17–24, August 2–8, and September 9–15 for 2011, and June 20–29, July 14–21, August 11–18, and September 8–15 for 2012. The Alaska DOT (Department of Transportation) maintains the access road from Nome to Council from late May to late September. Because this access road was closed during the snow-covered period (October to May), we could not conduct CO<sub>2</sub> efflux measurement during the non-growing season. The Council site has been managed by the WERC (Water Environmental Research Center) of UAF (University of Alaska Fairbanks) since 1999, for examining changes in permafrost and the water cycle (Yoshikawa and Hinzman, 2003).

This study determined CO<sub>2</sub> efflux and environmental factors in lichen-, moss-, and tussock-dominant tundra microsites within a 40 m × 40 m plot (5 m interval; 81 points) at this site during the growing seasons of 2011 and 2012. Our plot was established for better understanding of spatiotemporal variations of CO<sub>2</sub> efflux and environmental data. Within the 81-point area, dominant ground plants are lichen (*Cladonia mitis*, *Cladonia crispata*, and *Cladonia stellaris*); moss such as sphagnum (*Sphagnum magellanicum*, *Sphagnum angustifolium*, and *Sphagnum fuscum*) and others (*Polypodium* spp., *Thuidium abietinum*, and *Calliergon* spp.); and cotton grass tussock tundra (*Eriophorum vaginatum*). Dominant lichen, moss, and tussock tundra occupied 27, 53, and 20 % of the plot, respectively.

Soil temperatures were taken at 5 and 10 cm below the surface using a portable thermometer with two probes (Model 8402-20, Cole-Parmer, USA), and soil moisture was measured at each point with a portable soil-moisture logger (HH2, Delta-T Devices, UK) with sensor (ML2, Delta-T Devices, UK). Thaw depth was measured with a fiberglass tile probe (1.5 m long) and pH with a waterproof meter (IQ 160, Ben Meadows, USA) in September 2011 for soil characteristics. A one-way and two-way ANOVA (95 % confidence level) and data regression analysis using Microsoft Excel Data Analysis software were performed.

## 2.2 Estimation of CO<sub>2</sub> efflux

Our dynamic CO<sub>2</sub> efflux-measuring system was portable, convenient, and capable of calculating efflux in situ. The 81-cylinder chamber base (30 cm diameter, 40 cm height) was fixed to the surface at each point. This system consisted of a transparent-material chamber lid (35 cm diameter, 0.3 cm thickness) with input and output urethane tubing (6 mm OD; 4 mm ID) and a pressure vent, a commercial pump (CM-15-12, Enomoto Micro Pump Co., Ltd., Japan), an NDIR CO<sub>2</sub> analyzer (LI-820, LI-COR Inc., USA), a commercial 12 V battery, and a laptop computer for efflux calculation (Kim et al., 2013). This system is similar to the manual system by Savage and Davidson (2003; see Fig. 1). To minimize the effect of pressure inside the chamber, the flow rate of the pump was maintained at 0.5 L min<sup>−1</sup> due to the under- or overestimation of CO<sub>2</sub> efflux by under- or over-pressurization of the chamber used and caused by flow restrictions in air circulation design (Davidson et al., 2002). Efflux-measuring time was on a 5–10 min interval, depending on weather and soil surface conditions. For tussock CO<sub>2</sub> efflux estimates, the surface area was variable and dependent on height; average tussock height in this case was  $18.7 \pm 5.1$  cm (CV: 27 %).

Efflux was calculated from the following equation, as described by Kim et al. (2013):

$$F_{\text{CO}_2} = \rho_a \times (C/t) \times (V/A), \quad (1)$$

where  $F_{\text{CO}_2}$  represents measured soil CO<sub>2</sub> efflux (g CO<sub>2</sub> m<sup>−2</sup> min<sup>−1</sup>),  $\rho_a$  is the molar density of dry air (mol m<sup>−3</sup>),  $C$  (ppmv) is the change in CO<sub>2</sub> concentrations during measuring time ( $t$ , 5 to 10 min),  $V$  is chamber volume, and  $A$  is surface area (cross section = 0.070 m<sup>2</sup>). The height of each chamber was also measured alongside the chamber to allow calculation of the efflux.

To assess the response of temperature dependence on CO<sub>2</sub> efflux, the relationship was plotted, showing exponential curves for soil temperature at depths of 5 and 10 cm from this equation:

$$F_{\text{CO}_2} = \beta_0 \times e^{\beta_1 \times T}, \quad (2)$$

where  $T$  is soil temperature (°C) and  $\beta_0$  and  $\beta_1$  are constants. This exponential relationship is commonly used to represent soil carbon efflux as a function of temperature (Davidson et al., 1998; Xu and Qi, 2001; Davidson and Janssens, 2006; Rayment and Jarvis, 2000; Kim et al., 2007, 2013).  $Q_{10}$  temperature coefficient values were calculated as in Davidson et al. (1998) and Kim et al. (2013):

$$Q_{10} = e^{\beta_1 \times 10} \quad (3)$$

$Q_{10}$  is a measure of the change in reaction rate at intervals of 10 °C, based on Van 't Hoff's empirical rule that a rate increase on the order of 2–3 times occurs for every 10 °C rise in temperature (Lloyd and Taylor, 1994).

### 2.3 Description of Hierarchical Bayesian (HB) model

To evaluate the relationship between CO<sub>2</sub> efflux and environmental variables, we modeled observed CO<sub>2</sub> efflux using an HB model with four explanatory variables: soil temperature (ST), soil moisture (SM), vegetation types (Vege), and thaw depth (THAW).

First, CO<sub>2</sub> efflux ( $F_{CO_2}$ ) was assumed normally distributed with mean parameter ( $\mu_{flux}$ ) and variance parameter ( $\sigma$ ):

$$F_{CO_2} \sim \text{normal}(\mu_{flux}, \sigma^2). \quad (4)$$

The scale parameter ( $\mu_{flux}$ ) was determined from the following equation:

$$\mu_{flux} = f_P \cdot f_{ST} \cdot f_{SM} \cdot f_{THAW}, \quad (5)$$

where  $f_P$  represents the function of CO<sub>2</sub> efflux potential,  $f_T$  and  $f_{SM}$  are limiting response functions, ranging from 0 to 1.  $f_P$  was defined as follows:

$$f_P = \beta_0 + \text{vege}_{[k]} + \text{year}_{[l]} + \text{posi}_{[ij]}, \quad (6)$$

in which  $f_P$  is a linear predictor with intercept ( $\beta_0$ ) and three random effects (vege, year, and posi). The Posi term represents the spatial random effect of the conditional autoregressive model (CAR) proposed by Besag et al. (1991).

Temperature ( $f_T$ ) uses a modified Van 't Hoff equation as follows:

$$f_{ST} = e^{\frac{ST - ST_{ref}}{10} \log(Q_{10})}, \quad (7)$$

where  $f_{ST}$  is the temperature response function, varying from 0 to 1. The explanatory variable of this function, represented by ST and  $ST_{ref}$ , is a constant, set at 25 °C for this study. The temperature sensitivity parameter is shown by  $Q_{10}$ . The soil moisture limiting function ( $f_{SM}$ ) is defined as follows:

$$f_{SM} = \left( \frac{SM - a}{b - a} \right)^a \left( \frac{SM - c}{b - c} \right)^{-d(b-c)/(b-a)}, \quad (8)$$

where the soil moisture response function,  $f_{SM}$ , ranges from 0 to 1 and is the same as the temperature response function (Hashimoto et al., 2010). Soil moisture is the explanatory variable of this function, and  $a$ ,  $b$ ,  $c$ , and  $d$  are the parameters for determining the shape of the soil moisture function. The function has a convex shape, and values range from 0 to 1. Parameters  $a$  and  $c$  are the minimum and maximum values of SM, respectively (i.e.,  $g(a) = g(c) = 0$ ). Parameter  $b$ , which ranges between  $a$  and  $c$ , is the optimum parameter (i.e.,  $g(b) = 1$ ). Parameter  $d$  controls the curvature of the function, though the three other parameters also affect the shape. This function was adopted from the DAYCENT model (Parton et al., 1996; Del Grosso et al., 2000).

$f_{THAW}$  is a function of thaw depth. We modeled this as follows:

$$f_{THAW} = \frac{1}{1 + e^{k-r \cdot THAW}}, \quad (9)$$

where the thaw depth function also ranges from 0 to 1. THAW is the explanatory variable of this function, and  $k$  and  $r$  are the parameters. We assumed CO<sub>2</sub> efflux to monotonically increase together with thaw depth (depth of active layer); however, these increases are not simply proportional, due to carbon depth distribution.

Finally, we modeled the priors of each parameter. For vegetation, we incorporated a random effect as follows:

$$\text{Vege}_k \sim \text{normal}(0, \sigma_{vege}), \quad (10)$$

$$\text{Year}_l \sim \text{normal}(0, \sigma_{year}). \quad (11)$$

For spatially explicit random effect, we used CAR modeling (Besag et al., 1991) as follows:

$$\text{Posi}_{ij} \sim \text{normal}(b_{ij}, \frac{\sigma_{\text{posi}_{ij}}}{n}), \quad (12)$$

$$b_{ij} \sim \frac{1}{n_{ij}} \sum_{m=1}^{\text{neighbors}(ij)} b_m, \quad (13)$$

where  $n_{ij}$  is the number of neighbors for neighborhood  $ij$ .

For priors, we defined as follows:

$$\begin{aligned} \beta_0 &\sim \text{normal}(0, 1000), \\ Q_{10} &\sim \text{uniform}(1, 10), \\ a &\sim \text{uniform}(-2, 0), \\ b &\sim \text{uniform}(0.1, 0.5), \\ c &\sim \text{uniform}(1, 3), \\ d &\sim \text{uniform}(0.01, 10), \\ k &\sim \text{uniform}(0, 10), \\ r &\sim \text{uniform}(0, 1), \\ \sigma^2 &\sim \text{uniform}(0, 100), \\ \sigma_{vege}^2 &\sim \text{uniform}(0, 100), \\ \sigma_{year}^2 &\sim \text{uniform}(0, 100). \end{aligned} \quad (14)$$

For  $\beta_0$ , we used a normal distribution with mean 0 and a very large variance. Priors regarding soil moisture function ( $a$ ,  $b$ ,  $c$ ,  $d$ ) are based on Hashimoto et al. (2012). We set priors for  $\sigma_{vege}^2$  and  $\sigma_{year}^2$  to be vague, meaning large enough in value to accommodate the actual observed CO<sub>2</sub> efflux of this study.

The joint posterior probability is described as follows:

$$\begin{aligned} p(\theta | \text{data}) &\propto \prod \text{Normal}(F_{CO_2} | \mu, \beta_0, 10, a, b, c, d, k, r, \\ &\quad \sigma_1, \sigma_{vege}, \sigma_{year}, \sigma_{posi}) \times p(\beta_0) \times p(Q_{10}) \\ &\quad \times p(a) \times p(b) \times p(c) \times p(d) \times p(k) \times p(r) \\ &\quad \times p(\sigma_1) \times p(\sigma_{vege}) \times p(\sigma_{year}) \times p(\sigma_{posi}), \end{aligned} \quad (15)$$

where  $p(\theta)$  denotes priors. For this model, we used MCMC methods implemented with Bayesian inference using the Gibbs sampling software WinBUGS (WinBUGS, version 1.4.3; D. Spiegelhalter et al., 2007, available at <http://www>).

src-bu.ac.uk/bugs), and the Gelman–Rubin convergence diagnostic as an index. For the model, we ran 20 000 Gibbs sampler iterations for three chains, with a thinning interval of 10 iterations. We discarded the first 10 000 iterations as burn-in, and used the remaining iterations to calculate posterior estimates. R was used to call JAGS/WinBUGS and calculate statistics in R.

### 3 Results and discussion

#### 3.1 CO<sub>2</sub> efflux and environmental factors

Table 1 shows monthly average  $\pm$  standard deviation (coefficient of variance, %) of CO<sub>2</sub> efflux, soil temperature at 5 and 10 cm below the surface, soil moisture, thaw depth, and pH in lichen, moss, tussock tundra, and grass during the growing seasons of 2011 and 2012. Annual growing-season-average CO<sub>2</sub> efflux is  $4.6 \pm 2.5$  mg CO<sub>2</sub> m<sup>-2</sup> min<sup>-1</sup> (54 %) and  $3.1 \pm 2.0$  mg CO<sub>2</sub> m<sup>-2</sup> min<sup>-1</sup> (66 %) for 2011 and 2012, respectively. This indicates that growing season CO<sub>2</sub> efflux in 2011 was 1.5 times higher than in 2012, as well as the significance of heavy rainfall during the middle of the growing season of 2012. CO<sub>2</sub> efflux in tussock tundra was approximately 1.8 times greater than in other plants, which may be due more to tussock's relatively wider surface area than others. While surface area in lichen and moss is 0.070 m<sup>2</sup> – the same surface area of the measurement chamber – average surface area of tussock is  $0.090 \pm 0.024$  m<sup>2</sup>, based on an average height of  $19.2 \pm 5.1$  cm. CO<sub>2</sub> efflux in the Arctic tundra of Alaska ranged from 0.38 to 1.6 mg CO<sub>2</sub> m<sup>-2</sup> min<sup>-1</sup> in lichen and 0.44 to 4.3 mg CO<sub>2</sub> m<sup>-2</sup> min<sup>-1</sup> in tussock during the growing season (Poole and Miller, 1982). Within tundra near Barrow, Alaska, meanwhile, CO<sub>2</sub> efflux in tussock and wet sedge was 0.23 and 0.022 mg CO<sub>2</sub> m<sup>-2</sup> min<sup>-1</sup>, respectively (Oechel et al., 1997), suggesting that CO<sub>2</sub> efflux in tussock is indeed a more significant atmospheric CO<sub>2</sub> source than wet sedge. Kim et al. (2013) reported that tussock is an important source of carbon efflux into the atmosphere, contributing 3.4-fold more than other vegetation types in Alaska tundra and boreal forest systems. Further, tussock-originated CO<sub>2</sub> efflux, which occupies a circumpolar area ranging from  $9 \times 10^{11}$  m<sup>2</sup> (Miller et al., 1983) to  $6.5 \times 10^{12}$  m<sup>2</sup> (Whalen and Reeburgh, 1988) when counted with moss species, provides a quantitative understanding of a significant atmospheric carbon source from the Arctic terrestrial ecosystem. Considering the circumpolar distribution of tussock tundra and moss in the Arctic tundra ecosystem, CO<sub>2</sub> efflux measured in this study should not be overlooked in the evaluation of the regional/global carbon budget regarding distribution characteristics of ground plants.

The spatial distribution of CO<sub>2</sub> efflux within a 40 m  $\times$  40 m plot in 2011 and 2012 is shown in Fig. 2. CO<sub>2</sub> efflux in June 2011 was much higher than during other observation periods, reflecting the effects of higher air

temperature and lower precipitation in June (see Fig. 1). This further suggests an explicit difference in CO<sub>2</sub> efflux between June of 2011 and June 2012 within the plot, as shown in Table 1. We also note that CO<sub>2</sub> efflux in September 2012 rapidly decreased due to heavy rainfall from mid-August to mid-September 2012. Within the plot, while the CV of monthly average CO<sub>2</sub> efflux in 2011 was prone to decrease, CV in 2012 tends to increase. This denotes the extremely environmental and meteorological changes in 2012 compared to 2011.

Annual growing season average and standard deviation for soil temperatures at 5 and 10 cm below the soil surface were  $9.0 \pm 4.2$  °C (47 %) and  $5.9 \pm 3.9$  °C (66 %) for 2011 and  $7.7 \pm 4.5$  °C (58 %) and  $5.7 \pm 3.5$  °C (61 %) for 2012, respectively. This indicates that soil temperature in 2011 was higher than in 2012, similar to annual average CO<sub>2</sub> efflux, suggesting soil temperature is likely to modulate CO<sub>2</sub> efflux, as largely reported in regions worldwide (Davidson et al., 1998; Xu and Qi, 2001; Davidson and Janssens, 2006; Rayment and Jarvis, 2000; Kim et al., 2007, 2013). The spatial distribution of high/low soil temperature for each month was identical to the pattern of high/low CO<sub>2</sub> efflux, as also shown in Fig. 2.

Annual average soil moisture was  $0.253 \pm 0.158$  m<sup>3</sup> m<sup>-3</sup> (CV: 62 %) in 2011 and  $0.272 \pm 0.180$  m<sup>3</sup> m<sup>-3</sup> (66 %) in 2012, indicating moisture in 2011 was slightly lower than in 2012. Soil moisture in September 2011 was not measured, due to damage to the soil moisture sensor. Spatial distribution of soil moisture is related to geographical topography, such as slope and relief within the plot, reflecting spatial distribution of lower CO<sub>2</sub> efflux and lower soil temperature in the trough area (not shown). Soil moisture, along with soil temperature, is also an important factor in the control of CO<sub>2</sub> efflux (Davidson et al., 1998; Gaumont-Guay et al., 2006; Mahecha et al., 2010; Kim et al., 2013).

Average thaw depth was  $39 \pm 5$  cm (15 %) in 2011 and  $38 \pm 6$  cm (15 %) in 2012, showing no significant difference, based on a one-way ANOVA at the 95 % confidence level ( $p < 0.001$ ). The distribution of thaw depth (not shown) appears similar to the soil moisture pattern, which is inversely related to CO<sub>2</sub> efflux and soil temperature. The average thaw rate over our 81 points was 0.43 cm day<sup>-1</sup> in 2011 and 0.41 cm day<sup>-1</sup> in 2012, reflecting that thaw rate over time remains almost constant during the growing season, and that thaw depth is not considered to regulate CO<sub>2</sub> efflux. In general, the deeper the active layer in response to permafrost thaw in the Arctic (Marchenko et al., 2008), the greater the CO<sub>2</sub> emissions from the soil into the atmosphere (Elberling et al., 2013), also suggesting the potential decomposition of frozen, higher-stocked soil organic carbon (Ping et al., 2008; Tarnocai et al., 2009; Grosse et al., 2011). However, temporal variation in thaw depth of the active layer may not stimulate CO<sub>2</sub> production. This suggests that the strength of CO<sub>2</sub> production that depends on soil microbial metabolism is affected more by environmental factors than constant active

**Table 1.** Average and standard deviation (coefficient of variation, %) of CO<sub>2</sub> efflux, soil temperature at 5 and 10 cm below the surface, soil moisture, thaw depth, and pH in lichen, moss, and tussock tundra in Council, Seward Peninsula, Alaska during growing seasons of 2011 and 2012.

Month	Vegetation	<i>n</i>	CO <sub>2</sub> efflux (mg CO <sub>2</sub> m <sup>-2</sup> min <sup>-1</sup> )	Soil temperature (°C)		Soil moisture (m <sup>3</sup> m <sup>-3</sup> )	Thaw depth (cm)	pH
				5 cm	10 cm			
June, 2011	Lichen	22	5.7 ± 3.6 (63)	10.1 ± 2.5 (25)	3.3 ± 1.4 (42)	0.270 ± 0.162 (60)	22 ± 3 (12)	n.m.***
	Moss	43	7.8 ± 2.2 (29)	13.2 ± 2.9 (22)	6.7 ± 2.8 (42)	0.224 ± 0.122 (54)	21 ± 3 (14)	n.m.
	Tussock	16	12.9 ± 6.2 (48)	12.7 ± 3.3 (26)	7.6 ± 3.7 (48)	0.301 ± 0.116 (39)	22 ± 2 (11)	n.m.
	Average	81*	8.0 ± 3.6 (45)	12.3 ± 3.2 (53)	6.0 ± 3.1 (51)	0.255 ± 0.127 (49)	21 ± 3 (14)	
August, 2011	Lichen	24	2.5 ± 1.2 (47)	6.9 ± 1.5 (22)	4.4 ± 1.1 (25)	0.297 ± 0.200 (67)	38 ± 5 (14)	n.m.
	Moss	41	3.3 ± 1.7 (52)	9.0 ± 1.6 (18)	6.2 ± 1.7 (27)	0.264 ± 0.237 (90)	41 ± 8 (19)	n.m.
	Tussock	16	5.1 ± 2.7 (53)	9.4 ± 2.4 (25)	7.0 ± 2.1 (30)	0.256 ± 0.141 (55)	40 ± 5 (12)	n.m.
	Average	81*	3.3 ± 1.3 (39)	8.6 ± 1.9 (22)	5.8 ± 1.4 (24)	0.272 ± 0.180 (66)	40 ± 6 (15)	
September, 2011	Lichen	23	2.3 ± 0.9 (40)	6.2 ± 1.0 (16)	4.6 ± 1.0 (21)	– **	57 ± 8 (13)	3.7 ± 0.4 (7)
	Moss	43	2.5 ± 1.2 (50)	6.9 ± 1.4 (20)	5.6 ± 1.3 (23)	–	58 ± 12 (20)	3.8 ± 0.4 (11)
	Tussock	15	3.5 ± 1.5 (43)	6.5 ± 1.4 (22)	5.2 ± 1.3 (25)	–	55 ± 5 (8)	3.8 ± 0.3 (8)
	Average	81*	2.6 ± 0.8 (30)	6.0 ± 1.6 (26)	5.3 ± 1.1 (21)	–	57 ± 9 (16)	3.8 ± 0.4 (11)
June, 2012	Lichen	25	3.7 ± 2.0 (53)	11.1 ± 3.0 (27)	5.9 ± 2.6 (44)	0.213 ± 0.113 (53)	22 ± 3 (12)	– **
	Moss	38	4.7 ± 1.8 (39)	12.7 ± 2.4 (19)	7.1 ± 2.3 (32)	0.189 ± 0.097 (51)	21 ± 3 (16)	–
	Tussock	14	5.6 ± 1.9 (33)	12.2 ± 2.4 (19)	8.8 ± 2.5 (29)	0.339 ± 0.136 (40)	21 ± 2 (11)	–
	Grass	4	5.2 ± 2.1 (40)	10.4 ± 3.0 (28)	6.4 ± 2.1 (33)	0.304 ± 0.149 (49)	21 ± 2 (8)	–
Average	81*	4.8 ± 2.0 (42)	11.5 ± 2.6 (23)	6.6 ± 2.5 (38)	0.224 ± 0.125 (56)	21 ± 3 (14)		
July, 2012	Lichen	25	4.0 ± 1.5 (38)	10.1 ± 2.1 (21)	6.9 ± 1.8 (26)	0.165 ± 0.088 (53)	33 ± 3 (9)	– **
	Moss	38	4.3 ± 1.5 (35)	11.2 ± 2.4 (22)	7.9 ± 1.9 (25)	0.243 ± 0.086 (60)	31 ± 4 (13)	–
	Tussock	14	5.9 ± 2.8 (48)	10.5 ± 2.5 (23)	7.9 ± 2.5 (31)	0.268 ± 0.140 (52)	31 ± 2 (8)	–
	Grass	4	5.6 ± 1.9 (34)	9.9 ± 1.1 (11)	6.6 ± 1.0 (15)	0.208 ± 0.088 (42)	36 ± 6 (16)	–
Average	81*	5.0 ± 2.0 (40)	11.3 ± 2.2 (19)	7.2 ± 2.4 (33)	0.191 ± 0.118 (62)	33 ± 6 (18)		
August, 2012	Lichen	25	3.3 ± 1.1 (33)	13.0 ± 2.6 (20)	9.3 ± 2.2 (23)	0.201 ± 0.117 (58)	45 ± 4 (10)	– **
	Moss	38	4.7 ± 1.6 (35)	16.0 ± 2.5 (15)	11.9 ± 2.7 (22)	0.258 ± 0.115 (73)	44 ± 7 (15)	–
	Tussock	14	6.4 ± 2.1 (33)	16.2 ± 2.5 (15)	12.6 ± 4.0 (32)	0.288 ± 0.120 (42)	43 ± 3 (7)	–
	Grass	4	5.5 ± 2.4 (43)	13.2 ± 0.8 (6)	9.3 ± 1.2 (13)	0.199 ± 0.069 (35)	47 ± 11 (22)	–
Average	81*	4.8 ± 1.9 (40)	15.0 ± 2.9 (19)	11.0 ± 3.2 (29)	0.246 ± 0.126 (51)	45 ± 6 (13)		
September, 2012	Lichen	25	1.6 ± 0.9 (54)	3.5 ± 1.9 (55)	2.1 ± 1.6 (75)	0.465 ± 0.260 (56)	59 ± 7 (11)	– **
	Moss	38	1.8 ± 0.8 (44)	4.9 ± 2.3 (47)	3.1 ± 1.8 (59)	0.340 ± 0.264 (78)	60 ± 9 (16)	–
	Tussock	14	2.3 ± 1.0 (44)	5.9 ± 2.5 (42)	4.1 ± 2.0 (48)	0.427 ± 0.121 (28)	57 ± 4 (7)	–
	Grass	4	2.2 ± 0.9 (40)	2.9 ± 2.5 (26)	2.0 ± 1.6 (82)	0.456 ± 0.378 (82)	64 ± 9 (14)	–
Average	81*	1.9 ± 0.8 (42)	4.4 ± 2.2 (50)	2.7 ± 1.8 (65)	0.424 ± 0.262 (62)	60 ± 8 (13)		

\* denotes total measured points.

\*\* means not conducted.

\*\*\* indicates not measured.

layer depth for both years. The deeper active layer reached nearly 80 cm below the surface with the soil temperature profile at 50, 70, 80, and 92 cm from July 2012 to October 2013 (not shown). When the soil contained much higher soil moisture and much deeper thaw depth for September, pH presented a similar value of  $3.8 \pm 0.4$  (11%), representing an acidic tundra soil (pH < 5.5; Walker et al., 1998) in whole points. The pH measurement was not conducted during the growing season of 2012, due to near uniformity within the plot.

### 3.2 Environmental factors determining CO<sub>2</sub> efflux

CO<sub>2</sub> efflux is potentially modulated by environmental factors such as soil temperature, soil moisture, and thaw depth.  $Q_{10}$  values were calculated using Eq. (3), based on the exponential relationship between CO<sub>2</sub> efflux and soil temperature at 5 and 10 cm depths for each plant. Table 2 shows  $Q_{10}$  values and correlation coefficients between CO<sub>2</sub> efflux and soil temperature at 5 and 10 cm depths in lichen, moss, grass, and tussock tundra during the growing season, based on a one-way ANOVA with a 95% confidence level.  $Q_{10}$  is prone to increasing with time, suggesting that CO<sub>2</sub> production by

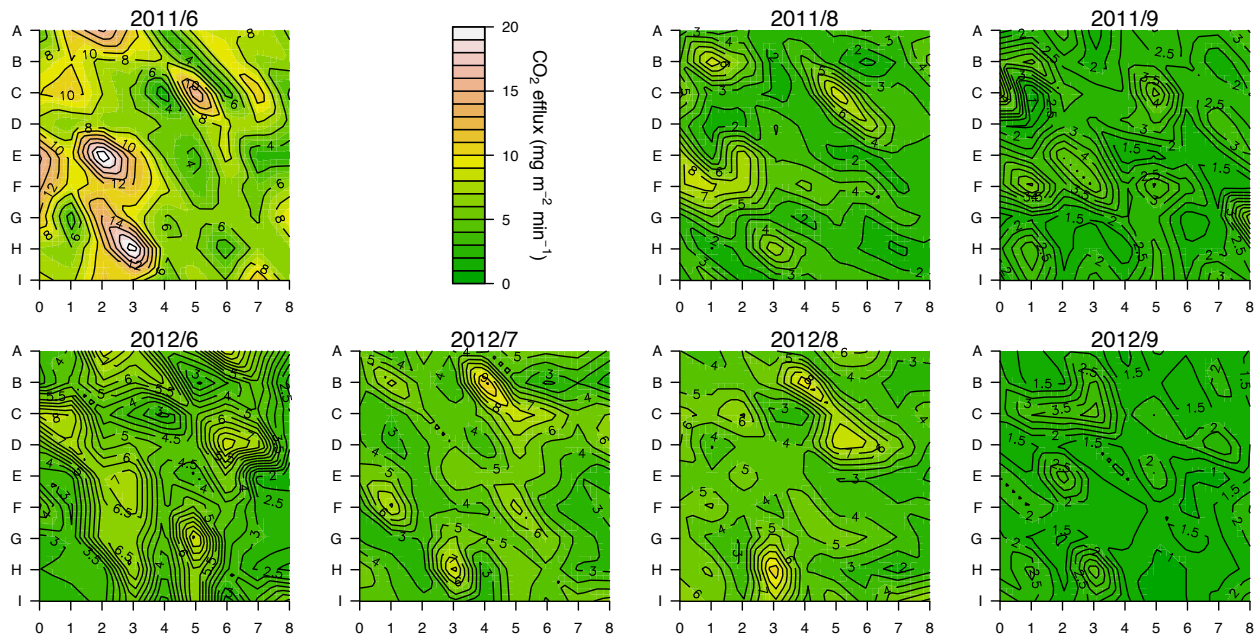


**Figure 2.** Spatial distribution of CO<sub>2</sub> efflux ( $\text{mg CO}_2 \text{ m}^{-2} \text{ min}^{-1}$ ) within a  $40 \text{ m} \times 40 \text{ m}$  plot (5 m interval; 81 points) in Council, Seward Peninsula, Alaska during the growing seasons of 2011 (upper panel) and 2012 (lower). Due to heavy rain in early July 2011, this data could not be measured, as shown in Fig. 1.

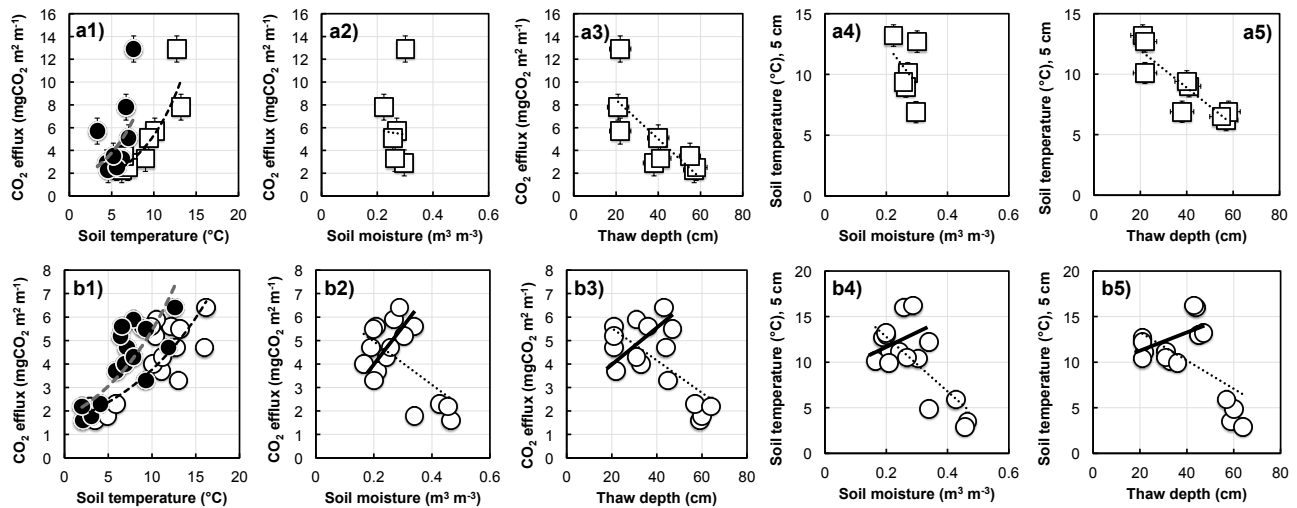
soil microbes and roots has greater sensitivity to a narrower range of soil temperatures, such as in the spring and fall seasons (Rayment and Jarvis, 2000; Gaumont-Guay et al., 2006; Monson et al., 2006; Malcom et al., 2009). In this Alaska tundra ecosystem, average daily CO<sub>2</sub> efflux from wet sedge followed soil surface temperature closely, increasing exponentially as soil surface temperature increased, while efflux from the tussock tundra ecosystem followed soil surface temperature nearly logarithmically (Oechel et al., 1997). In this study, the response from CO<sub>2</sub> efflux in tussock tundra to soil temperature depicts an almost linear relationship; however, it shows an exponential curve for  $Q_{10}$  values, listed in Table 2. Soil temperature at 5 cm depth explained 86 and 70 % of the variability in CO<sub>2</sub> efflux for 2011 and 2012, respectively, from the linear relationships, demonstrating that soil temperature is a significant factor in driving CO<sub>2</sub> efflux in dominant tundra plants during the growing season. The  $Q_{10}$  value for soil temperature at 5 cm depth for the moss regime in August 2012 was the lowest, at 1.15, resulting from higher soil temperature and higher soil moisture in August 2012 (Table 1).

Figure 3 shows the responses from monthly averaged CO<sub>2</sub> efflux to soil temperature at 5 and 10 cm depths (a1 and b1), soil moisture (a2 and b2), and thaw depth (a3 and b3), and the responses from soil temperature at 5 cm to soil moisture (a4 and b4) and thaw depth (a5 and b5) during the growing seasons of 2011 and 2012. Except for a1 and b1, these relationships were each negatively related during the growing season of 2011–2012. However, except for data measured in

September 2012, these relationships denoted positive lines from June to August 2012, as also shown in Fig. 3 (b2–5). This seems to be the effect of heavy rainfall beginning in 20 August 2012, as shown in Fig. 1, which represents daily and cumulative precipitation in 2011 and 2012. Interestingly, cumulative rainfall indeed began to surpass 2011 cumulative precipitation on 20 August 2012 (not shown). The correlation coefficient ( $R^2$ ) from June to August 2012 ranged from 0.01 in Fig. 3 (b3) to 0.32 in (b2). Hence, soil moisture elucidated 32 % of the variability in CO<sub>2</sub> efflux before the severe rainfall event of the fall season of 2012, demonstrating that soil moisture is another important factor aside from soil temperature. Jensen et al. (2014) estimated a CO<sub>2</sub> efflux of  $2.3 \pm 0.2$  and  $1.3 \pm 0.11 \text{ mg CO}_2 \text{ m}^{-2} \text{ min}^{-1}$  in the northwestern tundra of Alaska in July of 2011 and 2012, respectively, suggesting lower carbon flux results from the stronger rainfall event in 2012 (see Fig. 3a, Jensen et al., 2014), with a similar trend in air temperature between both years. This rainfall may have possibly inhibited 43 % of CO<sub>2</sub> emissions from the soil surface with increasing soil moisture in 2012, indicating a similar result to those observed in this study (Davidson et al., 1998).

### 3.3 Simulated CO<sub>2</sub> efflux from a hierarchical Bayesian model

We used 486 data sets of CO<sub>2</sub> efflux, soil temperature, soil moisture, vegetation types, and thaw depth for adjusting the parameters of a hierarchical Bayesian (HB) model, and the posterior distribution of the parameter for the CO<sub>2</sub> efflux is



**Figure 3.** Responses from monthly average CO<sub>2</sub> efflux to (1) average soil temperature at 5 and 10 cm (open and solid circles), (2) average soil moisture, and (3) thaw depth, as well as responses from average soil temperature at 5 cm to (4) average soil moisture and (5) average thaw depth during the growing seasons of (a) 2011 and (b) 2012. Dashed curves (a1 and b1) and dotted lines indicate the negatively linear relationship between the two. Furthermore, solid lines in b2–5 denote the positively linear relationship between factors, except for data measured in September.

summarized in Table 3. Potential CO<sub>2</sub> effluxes from the dominant plants calculated from posterior medians of the model were 16.8 mg CO<sub>2</sub> m<sup>-2</sup> min<sup>-1</sup> in grass (95 % predicted credible intervals (CI), 13.7–20.4 mg CO<sub>2</sub> m<sup>-2</sup> min<sup>-1</sup>), 15.3 mg CO<sub>2</sub> m<sup>-2</sup> min<sup>-1</sup> in lichen (95 % predicted CI, 11.1–16.8 mg CO<sub>2</sub> m<sup>-2</sup> min<sup>-1</sup>), 14.8 mg CO<sub>2</sub> m<sup>-2</sup> min<sup>-1</sup> in moss (95 % predicted CI, 10.2–15.9 mg CO<sub>2</sub> m<sup>-2</sup> min<sup>-1</sup>), and 21.9 mg CO<sub>2</sub> m<sup>-2</sup> min<sup>-1</sup> in tussock (95 % predicted CI, 24.0–31.0 mg CO<sub>2</sub> m<sup>-2</sup> min<sup>-1</sup>). This suggests that the contribution of atmospheric carbon from tussock tundra should receive attention when it comes to the tundra ecosystem and a circumpolar-scale response to the changing climate in the high Northern Hemisphere latitudes (Oechel et al., 1997; Bhatt et al., 2010, 2013; Kim et al., 2013). We computed limiting functions for soil temperature, soil moisture, and thaw depth of CO<sub>2</sub> efflux simulated by posterior distributions ( $n = 1000$ ), as shown in Fig. 4, for the quantitative assessment of the driving parameters for CO<sub>2</sub> efflux. Because changes in vegetation within the plot were not observed during this study period, these two parameters are not correlated with one another. In actuality, there was very low correlation ( $R^2 = 0.019$ ) between  $t_{\text{veg}}$  and  $t_{\text{year}}$  in our results.

For soil temperature limiting functions, the parameter simulated from the posterior median followed soil temperature nearly exponentially (Fig. 4a), demonstrating the definite temperature dependency of CO<sub>2</sub> efflux (Raich and Schlesinger, 1992; Davidson et al., 1998; Gaumont-Guay et al., 2006; Mahecha et al., 2010; Kim et al., 2013), as shown in Fig. 3a1 and b1. For soil temperature response, the parameter  $Q_{10}$  value was  $2.52 \pm 0.12$  (95 % predicted CI, 2.29–2.75).

For soil moisture limiting functions (Fig. 4b), the optimum soil moisture value was  $0.228 \text{ m}^3 \text{ m}^{-3}$  (95 % predicted CI,  $0.184\text{--}0.238 \text{ m}^3 \text{ m}^{-3}$ ). CO<sub>2</sub> efflux tended to increase with an increase in soil moisture when the soil moisture value was at the optimum, as shown in Fig. 3a2 and b2. On the other hand, the response from CO<sub>2</sub> efflux to soil moisture changed to a negative trend beyond the optimum value for soil moisture. The results from Jensen et al. (2014) proved the findings observed in this study, in which CO<sub>2</sub> efflux was relatively lower when soil moisture was much higher in 2012 than 2011, compared to 2011 (see Fig. 4b, Jensen et al., 2014). Davidson et al. (1998) reported a correlation between soil water content and CO<sub>2</sub> efflux in different drainage classes. CO<sub>2</sub> efflux increased when soil water content was less than  $0.2 \text{ m}^3 \text{ m}^{-3}$ ; on the other hand, higher soil moisture resulted in a decrease in CO<sub>2</sub> efflux (see Fig. 7, Davidson et al., 1998). For thaw depth limiting functions, the parameter increased to 20 cm, which represents the optimum thaw depth value (Fig. 4c). While CO<sub>2</sub> efflux increased with the rise in thaw depth in June until reaching the optimum thaw depth value, efflux was constant despite an increase in thaw depth with time. The response from CO<sub>2</sub> efflux to thaw depth turned to a negative trend during the growing seasons of 2011 and 2012, as shown in Fig. 3a3 and b3. These findings suggest that thaw depth may not be a significant parameter in influencing CO<sub>2</sub> efflux in the tundra ecosystem, in spite of a deeper active layer over time.

Spatial distribution of simulated CO<sub>2</sub> efflux, calculated from the posterior medians of the hierarchical Bayesian model during the growing seasons of 2011 and 2012, excluding July and September of 2011, is similar to that of

**Table 2.**  $Q_{10}$  values and correlation coefficient between CO<sub>2</sub> efflux and soil temperature at 5 and 10 cm below the soil surface in lichen, moss, and tussock during the growing season based on a one-way ANOVA with a 95 % confidence level.

Vegetation, Year	Month	5 cm			10 cm		
		$Q_{10}$	$R^2$	$p$	$Q_{10}$	$R^2$	$p$
Lichen, 2011	June	2.05	0.10	<0.001	1.68	0.01	0.018
	August	8.58	0.36	<0.001	2.47	0.04	<0.001
	September	10.59	0.43	<0.001	6.87	0.32	<0.001
	Total	4.97	0.34	<0.001	1.06	0.01	0.032
Moss, 2011	June	1.58	0.26	<0.001	1.54	0.15	0.073
	August	6.59	0.40	<0.001	5.88	0.41	<0.001
	September	7.54	0.28	<0.001	10.10	0.78	<0.001
	Total	5.05	0.62	<0.002	4.46	0.21	<0.001
Tussock, 2011	June	2.68	0.54	0.890	2.01	0.33	0.005
	August	8.66	0.68	<0.001	11.70	0.66	0.041
	September	10.74	0.58	<0.001	9.64	0.44	0.008
	Total	6.15	0.73	0.018	5.44	0.39	0.467
Lichen, 2012	June	4.03	0.66	<0.001	1.40	0.24	<0.001
	July	5.04	0.69	<0.001	0.57	0.65	<0.001
	August	2.41	0.46	<0.001	2.50	0.35	<0.001
	September	6.17	0.57	<0.001	9.55	0.59	<0.001
	Total	2.86	0.65	<0.001	1.09	0.19	<0.001
Moss, 2012	June	2.62	0.37	<0.001	0.95	0.01	<0.001
	July	3.82	0.66	<0.001	3.51	0.51	<0.001
	August	1.15	0.01	<0.001	1.14	0.01	<0.001
	September	2.10	0.16	<0.001	2.18	0.11	<0.001
	Total	2.44	0.54	<0.001	2.35	0.33	<0.001
Tussock, 2012	June	5.06	0.77	<0.001	4.59	0.68	<0.001
	July	3.78	0.73	<0.001	2.78	0.50	<0.001
	August	2.98	0.77	<0.001	1.59	0.37	<0.001
	September	4.12	0.72	<0.001	5.01	0.59	<0.001
	Total	3.11	0.76	<0.001	3.00	0.62	<0.001
Grass, 2012	Total	2.28	0.41	<0.001	3.11	0.38	<0.001

measured CO<sub>2</sub> efflux, as shown in Fig. 2. The pattern of simulated CO<sub>2</sub> efflux is nearly identical to the spatial distribution of measured CO<sub>2</sub> efflux (Fig. 3) as simulated CO<sub>2</sub> efflux is a function of soil temperature, soil moisture, and thaw depth. Of these, we consider soil temperature the most important parameter in modulating CO<sub>2</sub> efflux in the tundra ecosystem during the growing season. We compared measured CO<sub>2</sub> efflux to predicted CO<sub>2</sub> efflux using posterior medians in the HB model at each sampling period of 2011 and 2012 (Fig. 5), noting that CO<sub>2</sub> efflux simulated by a non-linear equation is consistent with measured data. Using the HB model, cumulative predicted CO<sub>2</sub> emission rates from 28 June to 30 September of 2011 and 2012 – based on monitored soil temperature and soil moisture in the Council area – were 742 g CO<sub>2</sub> m<sup>-2</sup> period<sup>-1</sup> (95 % predicted CI,

646–839 g CO<sub>2</sub> m<sup>-2</sup> period<sup>-1</sup>) and 539 g CO<sub>2</sub> m<sup>-2</sup> period<sup>-1</sup> (95 % predicted CI, 460–613 g CO<sub>2</sub> m<sup>-2</sup> period<sup>-1</sup>), respectively. These findings suggest that the 2012 CO<sub>2</sub> emission rate is constrained 27 % (95 % CI, 17–36 %) compared to the 2011 emission, demonstrating that higher soil moisture from severe rain constrains the emission of soil-produced CO<sub>2</sub> into the atmosphere (Jensen et al., 2014).

During the study periods (day-of-year; DOY: 179–273; Fig. 6) of 2011 and 2012, average soil temperature was  $9.3 \pm 3.8$  °C (CV: 41 %) and  $8.6 \pm 4.8$  °C, (CV: 56 %) respectively, showing that there is no significant difference between the years based on a one-way ANOVA 95 % confidence level. Trends in soil temperature during the periods of 2011 and 2012 were  $ST = -0.135 \times DOY + 5522$  ( $R^2 = 0.70$ ) and  $ST = -0.093 \times DOY + 3781$  ( $R^2 = 0.45$ ),

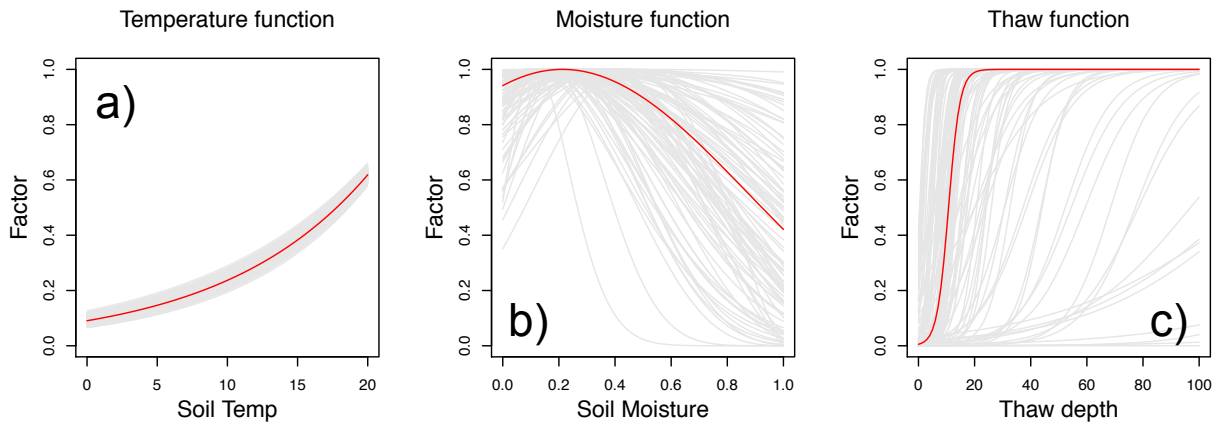


**Figure 4.** Limiting functions for (a) soil temperature, (b) soil moisture, and (c) thaw depth of CO<sub>2</sub> efflux simulated by posteriors ( $n = 1000$ ). Red solid lines are simulated from posterior median.

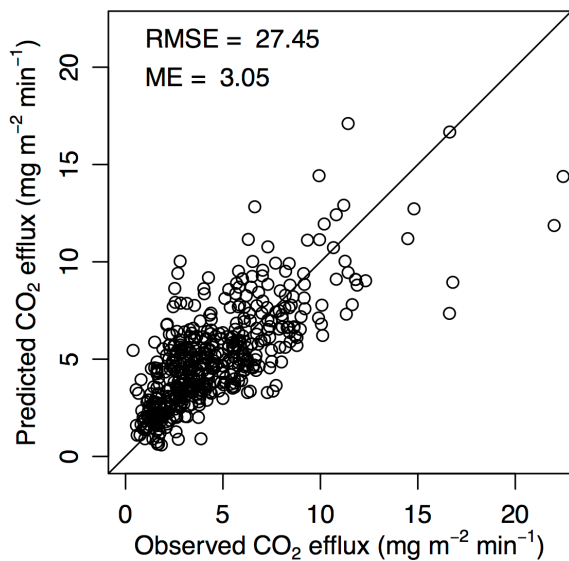


**Figure 5.** Response from measured CO<sub>2</sub> efflux to simulated CO<sub>2</sub> efflux by posterior medians in the HB model as a function of soil temperature, soil moisture, and thaw depth within a 40 m × 40 m plot (5 m interval; 81 points) in Council, Seward Peninsula, Alaska during the growing seasons of 2011 and 2012.

respectively. On the other hand, trends for soil moisture were  $SM = 0.0025 \times DOY - 103.5$  ( $R^2 = 0.37$ ) in 2011 and  $SM = -0.0008 \times DOY + 33.2$  ( $R^2 = 0.31$ ) in 2012, as shown in Fig. 6. Average soil moisture was  $0.260 \pm 0.040 \text{ m}^3 \text{ m}^{-3}$  (15 %) and  $0.493 \pm 0.124 \text{ m}^3 \text{ m}^{-3}$  (25 %) in 2011 and 2012, respectively, suggesting a distinct difference in soil moisture between the 2 years. Soil moisture during the 2012 period did not change with time, resulting from heavy rainfall events (Fig. 1) during the growing season (Jensen et al., 2014). When soil temperature at the end of September in 2012 was below zero (Fig. 6a), soil moisture sharply decreased, suggesting the frozen layer

**Table 3.** Summary of the posterior distribution from each parameter.

Parameter	Mean	S.D.	Upper			$R$ hat*
			2.5%	50.0%	97.5%	
$\beta_0$	16.79	4.22	8.72	17.01	25.16	1.01
$Q_{10}$	2.62	0.12	2.39	2.61	2.86	1.00
$a$	-1.27	0.49	-1.97	-1.34	-0.26	1.00
$b$	0.23	0.11	0.10	0.21	0.46	1.02
$c$	2.04	0.57	1.07	2.06	2.94	1.01
$d$	4.03	2.94	0.14	3.45	9.59	1.00
$e$	5.14	2.93	0.29	5.22	9.78	1.02
$f$	0.49	0.28	0.03	0.49	0.97	1.03
$\sigma_{\text{vege}}$	2.48	2.82	1.41	2.81	6.57	1.00
$\sigma_{\text{year}}$	4.28	4.58	2.36	4.87	14.07	1.00
$\sigma_{\text{posi}}$	2.36	1.93	1.16	3.01	5.64	1.02
$\sigma_1$	2.01	8.00	1.90	2.01	2.16	1.03

\*  $R$  hat denotes Gelman-Rubin convergence statistic. Values smaller than 1.1 indicate convergence of the estimated parameter.

reached the soil moisture measuring depth (e.g., near surface), as shown in Fig. 6b. The 2012 weather conditions may represent an episodic event, requiring additional monitoring for several representative points within the plot. Nevertheless, the higher CO<sub>2</sub> emission rate simulated by the HB model in 2011 is considered as likely the result of CO<sub>2</sub> efflux increasing until soil moisture reached optimum value, as shown in Fig. 4b. Therefore, soil moisture is an important parameter in constraining CO<sub>2</sub> emissions in this tundra ecosystem when the soil moisture is over the optimum value. When the annual simulated CO<sub>2</sub> emission rate was estimated from the relationship between CO<sub>2</sub> efflux and air temperature using Eq. (2), the annual emission rates were 827 and 609 g CO<sub>2</sub> m<sup>-2</sup> year<sup>-1</sup> in 2011 and 2012, respectively, corresponding to 86 and 80 % of annual CO<sub>2</sub> emission rates. Kim et al. (2013) estimated the growing season CO<sub>2</sub> emissions in the foothill tundra north of Brooks Range, Alaska to be 645 g CO<sub>2</sub> m<sup>-2</sup> period<sup>-1</sup> during 2006–2010, despite the

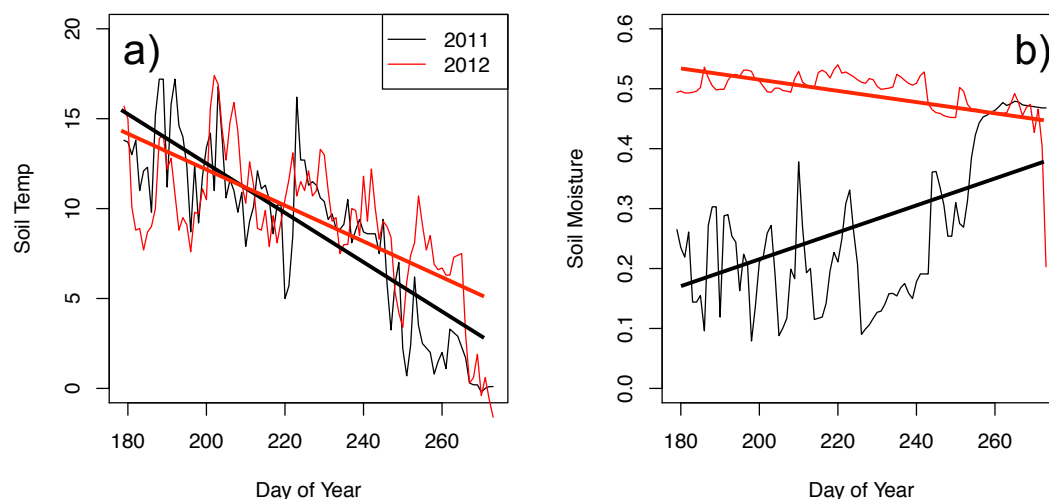


**Figure 6.** Temporal variations in (a) soil temperature (°C) and (b) soil moisture ( $\text{m}^3 \text{m}^{-3}$ ), measured for tundra sites during the growing seasons of 2011 (black) and 2012 (red). When soil temperature was below zero, at the end of September 2012, soil moisture dropped rapidly, as shown in Fig. 1.

difference in latitudinal distributions for CO<sub>2</sub> efflux and parameters. This value is situated between the 2011 and 2012 emission rates simulated for Council in this study. That is to say, the simulated CO<sub>2</sub> emission rates were 0.86 and 1.20 Mg CO<sub>2</sub> within a 40 m × 40 m plot during the growing seasons of 2012 and 2011, respectively.

#### 4 Summary and future works

Here, CO<sub>2</sub> efflux measurement was conducted with a manual chamber system in the tundra ecosystem of the Seward Peninsula of western Alaska, during the growing seasons of 2011 and 2012, to evaluate the significant parameter(s) controlling CO<sub>2</sub> efflux, as well as the effect(s) on the soil-produced CO<sub>2</sub> emission rate, using a hierarchical Bayesian (HB) model within a 40 m × 40 m plot (5 m interval; 81 points). Tussock tundra is an atmospheric carbon source in the tundra ecosystem year-round (Oechel et al., 1997; Kim et al., 2007, 2013). Considering the wide-ranged distribution of tussock in the high Northern Hemisphere latitudes, tussock- and moss-originated CO<sub>2</sub> efflux should not be overlooked as a significant carbon source in the estimation of regional and global carbon budgets. The response from CO<sub>2</sub> efflux in tussock to soil temperature showed a linear relationship; meanwhile, effluxes observed in lichen and moss regimes increased exponentially as soil temperature increased. This finding suggests that soil temperature is a key environmental factor in modulating CO<sub>2</sub> efflux, as many scientists have also reported around the world. Except for observations made in September 2012, soil moisture played an important factor in controlling CO<sub>2</sub> efflux. For 2012, higher soil moisture, resulting from the heavy rainfall in the end of August, was a constraining factor for the transport of soil-produced car-

bon into the atmosphere (Davidson et al., 1998; Jensen et al., 2014).

Using the HB model, we computed limiting functions for soil temperature, soil moisture, and thaw depth of CO<sub>2</sub> efflux simulated by posterior distribution. Simulated CO<sub>2</sub> efflux increased (1) exponentially as soil temperature increased and (2) nearly linearly until soil moisture reached optimum values ( $0.228 \text{ m}^3 \text{ m}^{-3}$ ); however, efflux decreased (3) logarithmically when soil moisture was beyond the optimum, and (4) nearly linearly until thaw depth was at optimum value (20 cm). Finally, efflux remained constant when thaw depth increased with time. These simulated findings show similar patterns to the data obtained in this study as well as the Jensen et al. (2014) results observed in the northwestern tundra of Alaska during the growing seasons of 2011 and 2012. During these growing seasons, the difference in soil temperature between the 2 years was not significant; however, there was a distinct difference in soil moisture between them, resulting in the inhibition of CO<sub>2</sub> emissions due to higher soil moisture. This demonstrates that higher soil moisture constrains 27 % of CO<sub>2</sub> emissions in 2012 compared to 2011. However, to prove the effect of soil moisture on controlling CO<sub>2</sub> emissions in the tundra ecosystem, additional studies must monitor the profiles of soil moisture and soil temperature at representative points from lichen, moss, and tussock tundra regimes within the plot. As conducted by Risk et al. (2011), the monitoring of soil CO<sub>2</sub> efflux must also show representative points, along with the monitoring of environmental factor profiles within the plot.

**The Supplement related to this article is available online at doi:10.5194/bg-11-5567-2014-supplement.**

**Acknowledgements.** This work was supported by a National Research Foundation of Korea grant funded by the South Korean Government (MSIP) (NRF-C1ABA001-2011-0021063) (Establishment of Circum-Arctic Permafrost Environment Change Monitoring Network and Future Prediction Techniques (CAPEC Project)). This research was conducted under the JAMSTEC-IARC Collaboration Study, with funding provided by the Japan Agency for Marine-Earth Science and Technology (JAMSTEC), as well as the IARC-JAXA Information System (IJIS), with funding partly provided by the Japan Aerospace Exploration Agency (JAXA) under a grant to the International Arctic Research Center (IARC). Finally, we would like to acknowledge the handling Editor (Y. Luo) and two anonymous reviewers significantly improved manuscript quality and readability.

Edited by: Y. Luo

## References

- ACIA (Arctic Climate Impact Assessment): Impacts of a Warming Arctic, Cambridge Univ. Press, Cambridge, UK, 146 pp., 2004.
- Besag, J., York, J. C., and Molife, A.: Bayesian image restoration with two applications in spatial statistics, *Ann. Inst. Stat. Math.*, 43, 1–59, 1991.
- Bhatt, U. S., Walker, D. A., Reynolds, M. K., Comiso, J. C., Epstein, H. E., Jia, G., Gens, R., Pinzon, J. E., Tucker, C. J., Tweedie, C. E., and Webber, P. J.: Circumpolar arctic tundra vegetation change is linked to sea ice decline, *Earth Interact.*, 14, 1–20, doi:10.1175/2010EI315.1, 2010.
- Bhatt, U. S., Walker, D. A., Reynolds, M. K., Bieniek, P. A., Epstein, H. E., Comis, J. C., Pinzon, J. E., Tucker, C. J., and Polyako, I. V.: Recent declines in warming and vegetation greening trends over pan-Arctic tundra, *Remote Sens.*, 5, 4229–4254, doi:10.3390/rs5094229, 2013.
- Bond-Lamberty, B. and Thomson, A.: Temperature-associated increases in the global soil respiration record, *Nature*, 464, 597–582, 2010.
- Clark, J. S.: Why environmental scientists are becoming Bayesians, *Ecol. Lett.*, 8, 2–14, doi:10.1111/j.1461-0248.2004.00702.x, 2005.
- Davidson, E. A. and Janssens, I. A.: Temperature sensitivity of soil carbon decomposition and feedback to climate change, *Nature*, 440, 165–173, 2006.
- Davidson, E. A., Belk, E., and Boone, R. D.: Soil water content and temperature as independent or confounded factors controlling soil respiration in a temperate mixed hardwood forest, *Glob. Change Biol.*, 4, 217–227, 1998.
- Davidson, E. A., Savage, K., Verchot, L. V., and Bavarri, R.: Minimizing artifacts and biases in chamber-based measurements of soil respiration, *Agr. Forest Meteorol.*, 113, 21–37, 2002.
- Del Grosso, S. J., Parton, W. J., Mosier, A. R., Ojima, D. S., Potter, C. S., Borken, W., Brumme, R., Butterbach-Bahl, K., Crill, P. M., Dobbie, K., and Smith, K. A.: General CH<sub>4</sub> oxidation model and comparisons of CH<sub>4</sub> oxidation in natural and managed systems, *Global Biogeochem. Cy.*, 14, 999–1019, 2000.
- Elberling, B. and Brandt, K. K.: Uncoupling of microbial CO<sub>2</sub> production and release in frozen soil and its implications for field studies of arctic C cycling, *Soil Biol. Biochem.*, 35, 263–272, 2003.
- Elberling, B., Michelsen, A., Schädel, C., Schuur, E. A. G., Christiansen, H. H., Berg, L., Tamstorf, M., and Sigsgaard, C.: Long-term CO<sub>2</sub> production flowing permafrost thaw, *Nat. Clim. Change*, 3, 890–894, doi:10.1038/nclimate1955, 2013.
- Gaumont-Guay, D., Black, T. A., Griffis, T. J., Barr, A. G., Jassal, R. A., and Nestic, Z.: Interpreting the dependence of soil respiration on soil temperature and water content in a boreal aspen stand, *Agr. Forest Meteorol.*, 140, 220–235, 2006.
- Grosse, G., Harden, J., Turetsky, M., McGuire, A. D., Camill, P., Tarnocai, C., Frolking, S., Schuur, E. A. G., Jorgenson, T., Marchenko, S., Romanovsky, V., Wickland, K. P., French, N., Waldrop, M., Bourgeau-Chaves, L., and Striegl, R. G.: Vulnerability of high-latitude soil organic carbon in North America to disturbance, *J. Geophys. Res.*, 116, G00K06, doi:10.1029/2010JG001507, 2011.
- Hashimoto, S., Morishita, T., Sakata, T., Ishizuka, S., Kaneko, S., and Takahashi, M.: Simple models for soil CO<sub>2</sub>, CH<sub>4</sub>, and N<sub>2</sub>O fluxes calibrated using a Bayesian approach and multi-site data, *Ecol. Model.*, 222, 1283–1292, 2011.
- Hinzman, L. D., Bettez, N. D., Bolton, W. R., Chapin, F. S., Dyurgerov, M. B., Fastie, C. L., Griffith, B., Hollister, R. D., Hope, A., Huntington, H. P., Jensen, A. M., Jia, G. J., Jorgenson, T., Kane, D. L., Klein, D. R., Kofinas, G., Lynch, A. H., Lloyd, A. H., McGuire, A. D., Nelson, F. E., Oechel, W. C., Osterkamp, T. E., Racine, C. H., Romanovsky, V. E., Stone, R. S., Stow, D. A., Sturm, M., Tweedie, C. E., Vourlitis, G. L., Walker, M. D., Walker, D. A., Webber, P. J., Welker, J. M., Winker, K. S., and Yoshikawa, K.: Evidence and implications of recent climate change in northern Alaska and other arctic regions, *Clim. Change* 72, 251–298, 2005.
- Hutchinson, G. L. and Livingston, P.: Soil-atmosphere gas exchange, in: *Methods of soil analysis: Part 4, Physical methods*, 3rd edn. Book Series 5, edited by: Dane, J. H. and Topp, G. C., Madison, WI, Soil Science Society of America, 1159–1182, 2002.
- Jensen, A. E., Lohse, K. A., Crosby, B. T., and Mora, C. I.: Variations in soil carbon dioxide efflux across a thaw slump chronosequence in northwestern Alaska, *Environ. Res. Lett.* 9, 025001, doi:10.1088/1748-9326/9/2/025001, 2014.
- Kim, Y., Ueyama, M., Nakagawa, F., Tsunogai, U., Tanaka, N., and Harazono, Y.: Assessment of winter fluxes of CO<sub>2</sub> and CH<sub>4</sub> in boreal forest soils of central Alaska estimated by the profile method and the chamber method: A diagnosis of methane emission and implications for the regional carbon budget, *Tellus B*, 59, 223–233, 2007.
- Kim, Y., Kim, S. D., Enomoto, H., Kushida, K., Kondoh, M., and Uchida, M.: Latitudinal distribution of soil CO<sub>2</sub> efflux and temperature along the Dalton Highway, Alaska. *Polar Sci.*, 7, 162–173, 2013.
- Koven, C. D., Ringeval, B., Friedlingstein, P., Ciais, P., Cadule, P., Khvorostyanov, D., Krinner, G., and Tarnocai, C.: Permafrost carbon-climate feedbacks accelerate global warming, *P. Natl. Acad. Sci. USA*, 108, 14769–14774, 2011.
- Lloyd, J. and Taylor, J. A.: On the temperature dependence of soil respiration, *Funct. Ecol.* 8, 315–323, 1994.
- Mahecha, M. D., Reichstein, M., Carvalhais, N., Lasslop, G., Lange, H., Seneviratne, S. I., Vargas, R., Ammann, C., Arain, M. A., Cescatti, A., Janssens, I. A., Migliavacca, M., Montagnani, L., and Richardson, A. D.: Global convergence in the tempera-

- ture sensitivity of respiration at ecosystem level, *Science*, 329, 838–840, doi:10.1126/science.1189587, 2010.
- Malcom, G. M., López-Gutiérrez, J., and Koide, R. T.: Temperature sensitivity of respiration differs among forest floor layers in a *Pinus resinosa* plantation, *Soil Biol. Biochem.*, 41, 1075–1079, 2009.
- Marchenko, S., Romanovsky, V., and Tipenko, G.: Numerical modeling of spatial permafrost dynamics in Alaska, in: Proceedings of the Ninth International Conference on Permafrost, edited by: Kane, D. L. and Hinkel, K. M., Inst. of North. Eng., Univ. of Alaska Fairbanks, Fairbanks, 1125–1130, 2008.
- Michaelson, G. J. and Ping, C. L.: Soil organic carbon and CO<sub>2</sub> respiration at subzero temperature in soils of Arctic Alaska, *J. Geophys. Res.*, 108, 8164, doi:10.1029/2001JD000920, 2003.
- Miller, P. C., Kendall, R., and Oechel, W. C.: Simulating carbon accumulation in northern ecosystems, *Simulation*, 40, 119–131, 1983.
- Monson, R. K., Lipson, D. L., Burns, S. P., Turnipseed, A. A., Delany, A. C., Williams, M. W., and Schmidt, S. K.: Winter forest soil respiration controlled by climate and microbial community composition, *Nature*, 439, doi:10.1038/nature04555, 2006.
- Nishina, K., Takenaka, C., and Ishizuka, S.: Spatial variations in nitrous oxide and nitric oxide emission potential on a slope of Japanese cedar (*Cryptomeria japonica*) forest, *Biogeochemistry*, 96, 163–175, 2009.
- Nishina, K., Akiyama, H., Nishimura, S., Sudo, S., and Yagi, K.: Evaluation of uncertainties in N<sub>2</sub>O and NO fluxes from agricultural soil using a hierarchical Bayesian model, *J. Geophys. Res.*, 117, G04008, doi:10.1029/2012JG002157, 2012.
- Oberbauer, S. F., Gillespie, C. T., Cheng, W., Gebauer, R., Sala Serra, A., and Tenhunen, J. D.: Environmental effects on CO<sub>2</sub> efflux from riparian tundra in the northern foothills of the Brooks Range, Alaska, USA, *Oecol.*, 92, 568–577, 1992.
- Oberbauer, S. F., Tweedie, C. E., Welker, J. M., Fahnestock, J. T., Henry, G. H. R., Webber, P. J., Hillister, R. D., Waler, M. D., Kuchy, A., Elmore, E., and Starr, G.: Tundra CO<sub>2</sub> fluxes in response to experimental warming across latitudinal and moisture gradients, *Ecol. Monogr.*, 72, 221–238, 2007.
- Oechel, W. C., Vourlitis, G., and Hastings, S. J.: Cold season CO<sub>2</sub> emissions from arctic soils, *Global Biogeochem. Cy.*, 11, 163–172, 1997.
- Oechel, W. C., Vourlitis, G., Hastings, S. J., Zulueta, R. C., Hinzman, L. D., and Kane, D.: Acclimation of ecosystem CO<sub>2</sub> exchange in the Alaska Arctic in response to decadal climate warming, *Nature*, 406, 978–981, 2000.
- Parton, W. J., Mosier, A. R., Ojima, D. S., Valentine, D. W., Schimel, D. S., Weier, K., and Kulmala, A. E.: Generalized model for N<sub>2</sub> and N<sub>2</sub>O production from nitrification and denitrification, *Global Biogeochem. Cy.*, 10, 401–412, 1996.
- Ping, C. L., Michaelson, G. J., Jorgenson, M. T., Kimble, J. H., Epstein, H., Romanovsky, V., and Walker, D. A.: High stock of soil organic carbon in the North American Arctic region, *Nat. Geosci.*, 1, 615–619, doi:10.1038/ngeo284, 2008.
- Poole, K. D. and Miller, P. C.: Carbon dioxide flux from three Arctic tundra types in North-Central Alaska, U.S.A., *Arctic Alp. Res.*, 14, 27–32, 1982.
- Post, E., Bhatt, U. S., Bitz, C. M., Brodie, J., Fulton, T. L., Hebblewhite, M., Kerby, J., Kutz, S., Stirling, J. K., and Walker, D. A.: Ecological consequences of Sea-ice decline, *Science*, 341, 519, doi:10.1126/science.1235225, 2013.
- R Development Core Team: A Language and Environment for Statistical Computing, R Found. Comput. Vienna, available at: <http://www.R-project.org/>, 2012.
- Raich, J. W. and Schlesinger, W. H.: The global carbon dioxide flux in soil respiration and its relationship to vegetation and climate, *Tellus B*, 44, 81–99, 1992.
- Rayment, M. B. and Jarvis, P. G.: Temporal and spatial variation of soil CO<sub>2</sub> efflux in a Canadian boreal forest, *Soil Biol. Biochem.*, 32, 35–45, 2000.
- Risk, D., Nickerson, N., Creelman, C., McArthur, G., and Owens, J.: Forced diffusion soil flux: A new technique for continuous monitoring of soil gas efflux, *Agr. Forest Meteorol.* 151, 1622–1631, 2011.
- Romanovsky, V., Burgess, M., Smith, S., Yoshikawa, K., and Brown, J.: Permafrost temperature records: indicators of climate change, *EOS Trans.*, 80, 589–594, 2002.
- Savage, K. E. and Davidson, E. A.: A comparison of manual and automated systems for soil CO<sub>2</sub> flux measurements: trade-offs between spatial and temporal resolution, *J. Exp. Bot.*, 54, 891–899, 2003.
- Schlesinger, W. H. and Andrews, J. A.: Soil respiration and the global carbon cycle, *Biogeochemistry*, 48, 7–20, 2000.
- Schuur, E. A. G., Vogel, J. G., Crummer, K. G., Lee, H., Sickman, J. O., and Osterkamp, T. E.: The effect of permafrost thaw on old carbon release and net carbon exchange from tundra, *Nature*, 459, 556–559, doi:10.1038/nature0803, 2009.
- Smith, L. C., Sheng, Y., MacDonal, G. M., and Hinzman, L. D.: Disappearing Arctic lakes, *Science*, 308, p. 1427, 2005.
- Spiegelhalter, D. T. A. and Best, N.: WinBUGS user manual, MRC Biostatistics Unit, Cambridge, UK, 2000.
- Sturm, M., J. Schimel, J., Michaelson, G., Welker, J. M., Oberbauer, S. F., Liston, G. E., Fahnestock, J., and Romanovsky, V.: Winter biological processes could help convert Arctic tundra to shrubland, *Bioscience*, 55, 17–26, 2005.
- Tarnocai, C., Canadell, J. G., Schuur, E. A. G., Kuhry, P., Mazhitova, G., and Zimov, S.: Soil organic carbon pools in the northern circumpolar permafrost region, *Global Biogeochem. Cy.*, 23, GB2023, doi:10.1029/2008GB003327, 2009.
- Walker, D. A., Auerbach, N. A., Bockheim, J. G., Chapin III, F. S., Eugster, W., King, J. Y., McFadden, J. P., Michaelson, G. J., Nelson, F. E., Oechel, W. C., Ping, C. L., Reeburg, W. S., Regli, S., Shiklomanov, N. I., Vourlitis, G. L.: Energy and trace-gas fluxes across a soil pH boundary in the Arctic, *Nature*, 394, 469–472, 1998.
- Walter, K. M., Smith, L. C., and Chapin, F. S.: Methane bubbling from northern lakes: present and future contributions to the global methane budget, *Philos. T. R. Soc. A.*, 365, 1657–1676, 2007.
- Whalen, S. C. and Reeburgh, W. S.: A methane flux time series for tundra environments, *Global Biogeochem. Cy.*, 5, 261–273, 1988.
- Xu, M. and Qi, Y.: Soil-surface CO<sub>2</sub> efflux and its spatial and temporal variations in a young ponderosa pine plantation in northern California, *Glob. Change Biol.*, 7, 667–677, 2001.
- Yoshikawa, K. and Hinzman, L. D.: Shrinking thermokarst ponds and groundwater dynamics in discontinuous permafrost near Council, Alaska, *Permafrost Periglac.*, 14, 151–160, 2003.